The edges evidence fusion to intensity channels in PolSAR image

Anderson A. de Borba
Dept. Engenharia Elétrica e Computação
UPM - Universidade Presbiteriana Mackenzie
IBMEC-SP
São Paulo, Brazil
anderson.borba@ibmec.edu.br

Maurício Marengoni
Dept. Engenharia Elétrica e Computação
UPM - Universidade Presbiteriana Mackenzie
São Paulo, Brazil
mauricio.marengoni@mackenzie.br

Alejandro C. Frery
Laboratório de Computação Científica e Análise Numérica - LACCAN
UFAL - Universidade Federal de Alagoas
Maceió, Brazil
acfrery@gmail.com

***Abstract*—Currently, it can be found several different methods for detection and fusion of edge evidence in the remote sensing research area. However, some of these methods, when applied to PolSAR images, produce inadequate results. In order to improve signal noise, there has been an investment in research with the use of statistical modeling. The present study proposes a method of detection and fusion of evidence edges based on the method of maximum likelihood, using a fusion of information by average, SWT, PCA, and ROC statistics. The precedents were applied to the intensity channels of a PolSAR real image. The results indicate a good performance of the method in detecting edges with possible paths for future research.**

***Index Terms*—PolSAR, edge detection, Maximum likelihood estimation, fusion methods**

I. Introduction

The paper presents some interring results on the detection and fusion of edge evidence, related to Synthetic Aperture Radar images (SAR) and in Synthetic Aperture Polarimetric radar images (PolSAR). In both cases, models and algorithms are required for appropriate treatment of their special characteristics.

There are several different edge detection techniques as electromagnetic modeling usage ([1]), estimate gradient based methods ([2]–[5]) and Markov's chains based technics ([6]) as well.

In [7] presents the comparison between several edge detectors, in wich some ideas of this work are described. Alternativelly, techniques based on statistical modeling have been used in edge detection in SAR images ([7]–[10]) and, currently, *Deep Learning* has been widely used in the remote sensing area ([11]–[14]).

The image fusion area is also explored in this work. A recent article, whose authors are [15], and, [16] show information about fusion techniques.

Grantee Capes/PROSUP/Mackenzie.

This paper will follow the statistical modeling approach, mainly the techniques described in [9], [17] using the Wishart distribution. To perform the fusion of information we have as a basis the references [16], [18].

The objective of this work is to detect edges in each channel of a PolSAR image and perform the fusion of the edge evidence, with the task of understanding the importance of the information of each one of these channels.

The article is structured as follows: in the section II describes the statistical modeling for PolSAR data, the modeling usage is presented in the sections III, IV and V, in the section VI the edge evidence methods with an emphasis on the ROC statistics-based method is described, some numerical results are shown and analyzed in section VII and, finally, in section VIII the concluding remarks are presented.

II. Statistical modeling for PolSAR data

Fully polarimetric SAR systems transmit orthogonally polarized microwave pulses and measure orthogonal components of the received signal. For each pixel, we have a matrix of scattering coefficients, which are complex numbers and describe the transformation from the transmitted electromagnetic field to the received electromagnetic field.

The transformation can be represented as

$$\begin{bmatrix} E_h^r \\ E_v^r \end{bmatrix} = \frac{e^{\hat{\imath}kr}}{r} \begin{bmatrix} S_{hh} & S_{hv} \\ S_{vh} & S_{vv} \end{bmatrix} \begin{bmatrix} E_h^t \\ E_v^t \end{bmatrix},$$

where k denotes the wave number, $\hat{\imath}$ is a complex number and r is the distance between the radar and the target. The electromagnetic field with components E_i^j has a subscribed index denoting horizontal (h) or vertical (v) polarization, while the superscript index indicates the received (r) or transmitted (t) wave. Defining $S_{i,j}$ as the complex scattering coefficients, such that the index i and j are associated with the reception and transmission of waves, for example, the scattering coeffi-

cient S_{hv} is associated with wave transmitted in the vertical direction (v) and received in the horizontal direction (h).

Being known each coefficient, the complex scattering matrix $\mathbf{S}$ is defined by

$$\mathbf{S} = \begin{bmatrix} S_{hh} & S_{hv} \\ S_{vh} & S_{vv} \end{bmatrix}, \quad (1)$$

and if the means of propagation of waves is reciprocal, then we will use the reciprocity theorem [19] to define the scattering matrix as being Hermitian. In this way, the scattering matrix can be represented by the vector

$$\mathbf{s} = \begin{bmatrix} S_{hh} \\ S_{hv} \\ S_{vv} \end{bmatrix}. \quad (2)$$

And considering the hypothesis that the distribution is circular Gaussian complex multivariate zero mean $N_3^C(0, \Sigma)$ ([20], [21]), whose the probability density function (pdf) is:

$$f_{\mathbf{s}}(\mathbf{s}; \mathbf{\Sigma}) = \frac{1}{\pi^3 |\mathbf{\Sigma}|} \exp(-\mathbf{s}^H \mathbf{\Sigma}^{-1} \mathbf{s}), \quad (3)$$

where $||cdot|$ is the determining matrix, the superscript index H denotes the conjugated complex number and $\mathbf{\Sigma}$ is the covariance matrix of the sample $\mathbf{s}$ such that $\mathbf{\Sigma} = E(\mathbf{s}\mathbf{s}^H)$.

As a result of the distribution being circular complex multivariate Gaussian with zero mean, and the entries for the $\mathbf{s}$ vector are $\mathbf{s}_{ij} = R_{ij} + iI_{ij}$, then due hypothesis it is required that R_{ij} and I_{ij} with $j = h, v$ satisfy

I- $E[R_{ij}] = E[I_{ij}] = 0$,
II- $E[R_{ij}^2] = E[I_{ij}^2]$,
II- $E[R_{ij} I_{ij}] = 0$,
IV- $E[R_{ij} R_{ij}] = E[I_{ij} I_{ij}]$,
V- $E[I_{ij} R_{ij}] = -E[R_{ij} I_{ij}]$.

where, $E[cdot]$ denotes the expected value.

The statistic modeling described was proven for polarimetric SAR data, confirming that it contains all the necessary information to characterize the backscatter, we found more information in [22] and [23].

The statistical modeling described so far deals only with single-sight modeling; however, polarimetric images are usually subjected to a multi-sighting process in order to improve the ratio between the signal and its noise. For this purpose, estimated positive hermitian defined matrices are obtained by computing the average of L independent targets of the same scene. Resulting in the estimated sample covariance matrix $\mathbf{Z}$ as [20], [24]

$$\mathbf{Z} = \frac{1}{L} \sum_{l=1}^{L} \mathbf{s}_l \mathbf{s}_l{}^H, \quad (4)$$

where $\mathbf{s}_l$ with $l = 1, \ldots, L$ samples of L complex vectors distributed as $\mathbf{s}$, so the sample covariance matrix associated with $\mathbf{s}_l$ denotes scattering for each sight L.

III. Multi-look Wishart density function

The multi-look process has the Wishart probability density function (pdf) defined by,

$$f_{\mathbf{Z}}(\mathbf{Z}; \mathbf{\Sigma}_{\mathbf{s}}, L) = \frac{L^{mL} |\mathbf{Z}|^{L-m}}{|\mathbf{\Sigma}_{\mathbf{s}}|^L \Gamma_m(L)} \exp(-L \operatorname{tr}(\mathbf{\Sigma}_{\mathbf{s}}{}^{-1} \mathbf{Z})), \quad (5)$$

where, $\operatorname{tr}(\cdot)$ is the trace operator of an array, $\Gamma_m(L)$ is a multivariate Gamma function defined by

$$\Gamma_m(L) = \pi^{\frac{1}{2}m(m-1)} \prod_{i=0}^{m-1} \Gamma(L - i)$$

and $\Gamma(\cdot)$ is the Gamma function and $m = 3$ for the present article. It can be said that $\mathbf{Z}$ is distributed as a Wishart distribution denoting for $\mathbf{Z} \sim W(\mathbf{\Sigma}_{\mathbf{s}}, L)$ and satisfying $E[\mathbf{Z}] = \mathbf{\Sigma}_{\mathbf{s}}$. Without loss of generality to the text, let is use the symbol $\mathbf{\Sigma}$ instead of $\mathbf{\Sigma}_{\mathbf{s}}$ to represent the covariance matrix associated with $\mathbf{S}$.

IV. Edge Detection

In the specialized literature, it is found a large offer of classical methods to detect edge, for example, Sobel, Canny, Laplacian da Gaussian (LoG) and LoG pyramidal. The classical edge detection methods are constructed assuming that noise is additive, which makes these methods inefficient for application in PolSAR images.

Based on the articles [8], [17], it is possible to propose an edge detection method for PolSAR images with multiple targets.The main idea is to detect the transition point in a thin a range, as possible, between two regions of the image. The transition point is defined as edge evidence. The noise in these types of images is the *speckle* type, and has multiplicative nature, making edge detection in SAR images a challenging task.

Edge detection methodologies occur in several stages, as follows:

1) identify the centroid of a region of interest (ROI) in an automatic, semi-automatic or manual manner;
2) to build centroid rays out of the area of interest;
3) to collect data on a neighbourhood around the rays using the *Bresenham's midpoint line algorithm*, ideally the size of a pixel;
4) detect points in the data range, which provide evidence of statistical property changes, i.e., a transition point that defines border evidence;
5) use the Generalized Simulated Anneling (GenSA) method, reference [25], to find maximum points in functions of interest;
6) fusion of evidence of detected edges in (hh), (hv) and vv channels.

V. Maximum Likelihood Method

The Maximum Likelihood Estimation (MLE) is a method estimates the parameters values of the model maximizing the data probability function, considering as known a data set and

a statistical model. More details on the likelihood concept can be found in [8], [17].

Suppose $\mathbf{X} = (X_1, X_2, \ldots, X_n)^T$ a random vector distributed according to the probability density function (pdf) $f(\mathbf{x}, \theta)$ with parameters $\theta = (\theta_1, \ldots, \theta_d)^T$ in the parameter space Θ, it is defined the likelihood function

$$L(\theta; \mathbf{X}) = \prod_{i=1}^{n} f(x_i; \theta),$$

and the logarithmic likelihood function, which is also called the log-likelihood function

$$l(\theta; \mathbf{X}) = \ln(L(\theta; \mathbf{X})) = \sum_{i=1}^{n} \ln(f(x_i; \theta)). \tag{6}$$

In a simplified form, the estimate of maximum likelihood can be written by

$$\widehat{\theta} = \arg \max_{\theta \in \Theta} L(\theta; \mathbf{x}),$$

and similarly

$$\widehat{\theta} = \arg \max_{\theta \in \Theta} l(\theta; \mathbf{x}).$$

Using the maximum likelihood method applied to the Wishart distribution, suppose $\mathbf{Z} = (\mathbf{Z}_1, \mathbf{Z}_2, \ldots, \mathbf{Z}_N)^T$ a random vector distributed according to the probability density function (pdf) (5) with parameters $\Sigma = \{\mathbf{\Sigma_A}, \mathbf{\Sigma_B}\}$ and L. The parameters $\mathbf{\Sigma_A}$, $\mathbf{\Sigma_B}$ belong to two different samples A and B, and the goal is to detect the border between the two samples.

The likelihood function of the sample described by (6) is given by the production equation of the density functions, respectively associated to each sample.

$$L(j) = \prod_{k=1}^{j} f_{\mathbf{Z}}(\mathbf{Z}_k^{'}; \mathbf{\Sigma_A}, L) \prod_{k=j+1}^{N} f_{\mathbf{Z}}(\mathbf{Z}_k^{'}; \mathbf{\Sigma_B}, L), \tag{7}$$

where $\mathbf{Z}_k^{'}$ is a possible approximation of the random matrix described in (4).

Using the equation (6), one has the log-likelihood function.

$$\begin{array}{rcl} l(j) = \ln L(j) & = & \sum_{k=1}^{j} \ln f_{\mathbf{Z}}(\mathbf{Z}_k^{'}; \mathbf{\Sigma_A}, L) \\ & + & \sum_{k=j+1}^{N} \ln f_{\mathbf{Z}}(\mathbf{Z}_k^{'}; \mathbf{\Sigma_B}, L). \end{array} \tag{8}$$

At this moment, we can perform algebraic manipulations in the probability density function in each term of the summation and replace in the two parts of the equation (6) resulting in

$$\begin{array}{rcl} l(j) & = & N\left[mL\ln\left(L\right) - \ln\left(\Gamma_m(L)\right)\right] \\ & - & L\left[j\ln\left(|\mathbf{\Sigma_A}|\right) + (N-j)\ln\left(|\mathbf{\Sigma_B}|\right)\right] \\ & + & (L-m)\sum_{k=1}^{N}\ln\left(|\mathbf{Z}_k^{'}|\right) \\ & - & L\left[\sum_{k=1}^{j} tr(\mathbf{\Sigma_A}^{-1}\mathbf{Z}_k^{'}) + \sum_{k=j+1}^{N} tr(\mathbf{\Sigma_B}^{-1}\mathbf{Z}_k^{'})\right]. \end{array} \tag{9}$$

The Σ matrix can be found using the maximum likelihood estimator denoted by $\widehat{\Sigma}$ according to the reference [20]. The equation (10) represents two estimates for the covariance matrix Σ that depend on the j position.

$$\widehat{\Sigma_I}(j) = \begin{cases} j^{-1}\sum_{k=1}^{j}\mathbf{Z}_k & \text{se} \quad I = A, \\ (N-j)^{-1}\sum_{k=j+1}^{N}\mathbf{Z}_k & \text{se} \quad I = B. \end{cases} \tag{10}$$

In the equation (9) we can replace the equation (10) and continue the algebraic manipulation, resulting in

$$\begin{array}{rcl} l(j) & = & N\left[-mL(1-\ln\left(L\right)) - \ln\left(\Gamma_m(L)\right)\right] \\ & - & L\left[j\ln\left(|\widehat{\mathbf{\Sigma}}_A(j)|\right) + (N-j)\ln\left(|\widehat{\mathbf{\Sigma}}_B(j)|\right)\right] \\ & + & (L-m)\sum_{k=1}^{N}\ln\left(|\mathbf{Z}_k^{'}|\right). \end{array} \tag{11}$$

The maximum argument $\widehat{j}_{ML}$ is edge evidence that will be used in fusion methods.

$$\widehat{j}_{ML} = \arg\max_{j} l(j).$$

VI. Methods of fusion of border evidence

A. Simple mean

The simple mean fusion method proposes the arithmetic mean of the edge evidence in each channel. The edge evidence fusion can be calculated by

$$IF(x, y) = \frac{1}{nc}\sum_{i=1}^{nc} IE_i(x, y), \tag{12}$$

where nc is the number of channels to be used in the fusion. We can get more details on the reference [18].

B. Stationary wavelet transform- SWT

This section is again based on the reference [26]. The SWT fusion method can be described by the following steps:

- calculate the SWT decomposition by getting L_{HH}, L_{HL}, L_{LH} and L_{LL} for each channel;
- in the decompositions L_{HH} the arithmetic mean of all channels, pixel by pixel, and in the decompositions L_{HL}, L_{LH} and L_{LL} is performed, is found the maximum between each channel, pixel by pixel, leaving a new decomposition $\bar{L}_{HH}$, $\bar{L}_{HL}$, $\bar{L}_{LH}$ and $\bar{L}_{LL}$;
- performing the reverse transformation of SWT, we get the image by fusing the edge evidence $IF(x, y)$.

C. Pincipal component analysis - (PCA)

This section is based on [26] and [18], where the PCA-based fusion method can be described by the following steps:

- organize the data in such a way that each image has a column vector, forming a Y matrix of dimension $l \times nc$, where $l = m \cdot n$, represents the multiplication of m lines and n columns of the matrices to be used in the fusion;
- calculate the average of the elements of these columns, generating a vector dimension of $1 \times nc$;
- subtract the average of each column from the Y matrix. Resulting in a X matrix of the same dimension of Y;
- find the C covariance matrix from X, calculating $C = XX^T$;

- calculate the eigenvalues Λ and the eigenvectors D, and sort the eigenvalues and eigenvectors in descending order. The matrices generated by the eigenvalues, on the main diagonal, and the eigenvectors placed in column, have dimensions $nc \times nc$;
- compute the components $P_i = \frac{V_i}{\sum_{i=1}^{l} V_i}$ with $i = 1, \ldots, nc$;
- we fuse $IF(x, y) = \sum_{i=1}^{nc} P_i IE_i(x, y)$. Remembering that the $\sum_{i=1}^{nc} P_i = 1$.

D. ROC statistics

The ROC statistical method was proposed and described in detail in the references [27] and [28]. The method describes a statistical model to obtain information automatically, from several images, or in several channels. The method can be described in the following procedures:

- obtain the evidence of edges in the channels, applying the method described in this article. Store this edge evidence in E_i matrices, with $i = 1, \cdots, nc$ in a binary way;
- define a V edge frequency matrix. The V matrix is generated by adding the evidence of E_i borders;
- use thresholds ranging from $t = 1, \ldots, nc$ generating M_t matrices;
- compare each M_t, fixed with all E_i, find the confusion matrix to generate the ROC curve. The point of the ROC curve that approaches (in the sense of the Euclidean distance) the diagnostic line, will have its threshold considered optimal;
- the M_t matrix, which corresponds to the threshold closest to the diagnostic line, is the fusion of edge evidence.

VII. Numerical results

The PolSAR image, with 4 looks of the Flevoland region in the Netherlands, was used for the numerical tests. The figure (1) shows the region of interest, where it was built the radial lines for edge detection.

Edge detection and subsequent evidence fusion were performed in this region of interest, in order to understand the weighting of each channel in the image formation.

In this study, edge detection was performed in the intensity channels (hh), (hv) and (vv), and subsequently, used for information fusion.

The figures 2 (a), (b) and (c) show, respectively, the edge evidence detection algorithms, applied to (hh), (hv) and (vv) channels.

The algorithm to detect evidence of edges worked well in the channels (hh) and (hv), achieving better accuracy in relation to the channel (vv).

In the canal (vv), edges that are not part of the homogeneous region of interest were detected, but are part of other edges of the image, researching the reason for this fact, we analyzed the function $l(j)$ and found that the function presents two peaks, representing possible evidence of edges, in which the largest was correctly detected.

The figures 3 (a) to (d) show, respectively, the fusion of evidence for the methods described in this article. In order, we list the method that shows the average of edge evidence, the method that uses the Stationary wavelet transform (SWT), the method that uses the Principal component analysis (PCA), and finally, the method based on ROC statistics.

The methods shown in the figures 3 (a), (b) and (c) use all the pixels detected in the different channels. Each method weighs the pixels in the different channels with their characteristics. The average also weighs the pixels. The (SWT) finds the coefficients of the linear combination of its wavelet bases, and the (PCA) weights the auto-vectors of the covariance matrix.

The ROC statistics method does not use all pixels of the channels, because the method is based on thresholds discarding pixels. This was observed in the figure 3(d).

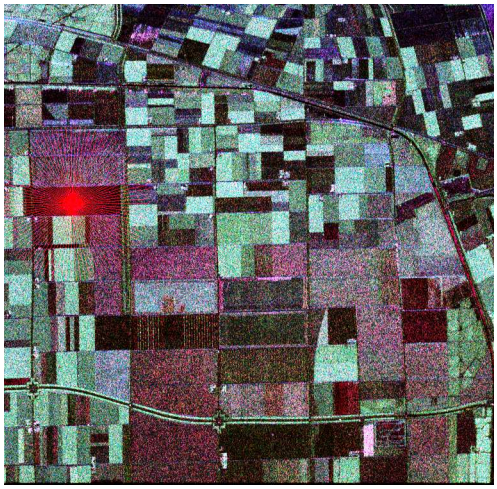

Fig. 1. Region of interest (ROI) in the image of Flavoland.

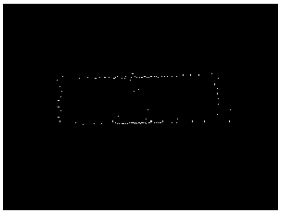

(a) Evidence in channel (hh)

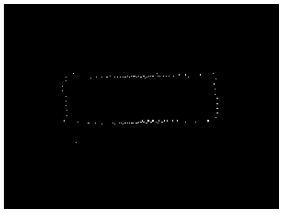

(b) Evidence in channel (hv)

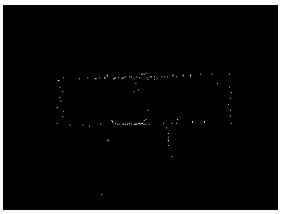

(c) Evidence in channel (vv)

Fig. 2. Dummy figure

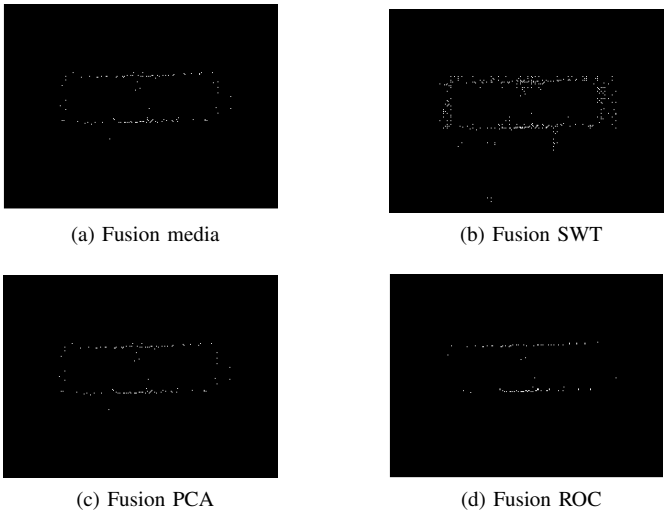

(a) Fusion media (b) Fusion SWT

(c) Fusion PCA (d) Fusion ROC

Fig. 3. Dummy figure

VIII. Conclusion

In this study, the statistical modelling approach was applied to real PolSAR data imaging. Aiming to understand the importance of information from each channel in the edge evidence fusions, the proposed algorithm was applied in three intensity channels (hh), (hv) and (vv). Initially, it was found the evidence of edges, using the maximum likelihood method in each channel, obtaining good results. After analyzed the results obtained in the three channels, it was observed that the method for the edge detections worked better in the channels (hh) and (hv) than the channel (vv), achieving a suitable accuracy.

Subsequently, the fusion of evidence of edges was performed with the methods of simple mean, SWT, PCA and ROC statistics. The first three methods performed well as shown in the results. The ROC statistics method suppressed several edge points, a behaviour expected because it is a method that uses thresholds; however, when applied in a larger number of channels, its performance tends to improve.

Based on these results, a possible way to improve them would be to increase the number of channels studied. This analysis open a way for future researches with application of different methods for edge evidence fusing.

References

[1] S. J. S. Sant'Anna, J. C. Da S. Lacava, and D. Fernandes, "From maxwell?s equations to polarimetric sar images: A simulation approach," *Sensors*, vol. 8, no. 11, pp. 7380–7409, 2008. [Online]. Available: http://www.mdpi.com/1424-8220/8/11/7380

[2] R. Touzi, A. Lopes, and P. Bousquet, "A statistical and geometrical edge detector for sar images," *IEEE Transactions on Geoscience and Remote Sensing*, vol. 26, no. 6, pp. 764–773, Nov 1988.

[3] C. J. Oliver, D. Blacknell, and R. G. White, "Optimum edge detection in sar," *IEE Proceedings - Radar, Sonar and Navigation*, vol. 143, no. 1, pp. 31–40, Feb 1996.

[4] R. Fjortoft, A. Lopes, P. Marthon, and E. Cubero-Castan, "An optimal multiedge detector for sar image segmentation," *IEEE Transactions on Geoscience and Remote Sensing*, vol. 36, no. 3, pp. 793–802, May 1998.

[5] X. Fu, H. You, and K. Fu, "A statistical approach to detect edges in sar images based on square successive difference of averages," *IEEE Geoscience and Remote Sensing Letters*, vol. 9, no. 6, pp. 1094–1098, Nov 2012.

[6] F. Baselice and G. Ferraioli, "Statistical edge detection in urban areas exploiting sar complex data," *IEEE Geoscience and Remote Sensing Letters*, vol. 9, no. 2, pp. 185–189, March 2012.

[7] E. Girón, A. C. Frery, and F. Cribari-Neto, "Nonparametric edge detection in speckled imagery," *Mathematics and Computers in Simulation*, vol. 82, no. 11, pp. 2182 – 2198, 2012. [Online]. Available: http://www.sciencedirect.com/science/article/pii/S037847541200136X

[8] J. Gambini, M. Mejail, J. Jacobo-Berlles, and A. C. Frery, "Feature extraction in speckled imagery using dynamic B-spline deformable contours under the G0 model," *International Journal of Remote Sensing*, vol. 27, no. 22, pp. 5037–5059, 2006.

[9] A. C. Frery, J. Jacobo-Berlles, J. Gambini, and M. Mejail, "Polarimetric SAR image segmentation with b-splines and a new statistical model," *CoRR*, vol. abs/1207.3944, 2012.

[10] M. Horritt, "A statistical active contour model for sar image segmentation," *Image and Vision Computing*, vol. 17, no. 3, pp. 213 – 224, 1999. [Online]. Available: http://www.sciencedirect.com/science/article/pii/S0262885698001012

[11] J. E. Ball, D. T. Anderson, and C. S. Chan, "A comprehensive survey of deep learning in remote sensing: Theories, tools and challenges for the community," *CoRR*, vol. abs/1709.00308, 2017. [Online]. Available: http://arxiv.org/abs/1709.00308

[12] X. X. Zhu, D. Tuia, L. Mou, G. Xia, L. Zhang, F. Xu, and F. Fraundorfer, "Deep learning in remote sensing: A comprehensive review and list of resources," *IEEE Geoscience and Remote Sensing Magazine*, vol. 5, no. 4, pp. 8–36, Dec 2017.

[13] J. Pont-Tuset, P. Arbeláez, J. T. Barron, F. Marques, and J. Malik, "Multiscale combinatorial grouping for image segmentation and object proposal generation," *IEEE Transactions on Pattern Analysis and Machine Intelligence*, vol. 39, no. 1, pp. 128–140, Jan 2017.

[14] S. Xie and Z. Tu, "Holistically-nested edge detection," *Int. J. Comput. Vision*, vol. 125, no. 1-3, pp. 3–18, Dec. 2017. [Online]. Available: https://doi.org/10.1007/s11263-017-1004-z

[15] A. Samat, P. Gamba, S. Liu, Z. Miao, E. Li, and J. Abuduwaili, "Quad-polsar data classification using modified random forest algorithms to map halophytic plants in arid areas," *Int. J. Applied Earth Observation and Geoinformation*, vol. 73, pp. 503–521, 2018. [Online]. Available: https://doi.org/10.1016/j.jag.2018.06.006

[16] A. Salentinig and P. Gamba, "A general framework for urban area extraction exploiting multiresolution sar data fusion," *IEEE Journal of Selected Topics in Applied Earth Observations and Remote Sensing*, vol. 9, no. 5, pp. 2009–2018, May 2016.

[17] A. Nascimento, M. Horta, A. Frery, and R. Cintra, "Comparing edge detection methods based on stochastic entropies and distances for polsar imagery," *Journal of Selected Topics in Applied Earth Observations and Remote Sensing*, vol. 7, no. 2, pp. 648–663, 2014.

[18] H. Mitchell, *Image Fusion: Theories, Techniques and Applications*. Springer Berlin Heidelberg, 2010. [Online]. Available: https://books.google.com.br/books?id=D7DXAX6eH2oC

[19] J.-S. Lee and E. Pottier, *Polarimetric radar imaging: from basics to applications*. CRC press, 2009.

[20] N. R. Goodman, "The distribution of the determinant of a complex wishart distributed matrix," *Ann. Math. Statist.*, vol. 34, no. 1, pp. 178–180, 03 1963. [Online]. Available: http://dx.doi.org/10.1214/aoms/1177704251

[21] J. S. Lee, K. W. Hoppel, S. A. Mango, and A. R. Miller, "Intensity and phase statistics of multilook polarimetric and interferometric SAR imagery," *IEEE Transactions on Geoscience and Remote Sensing*, vol. 32, no. 5, pp. 1017–1028, Sep. 1994.

[22] K. Sarabandi, "Derivation of phase statistics from the mueller matrix," *Radio Science*, vol. 27, 11 1992.

[23] C. López-Martínez, X. Fàbregas, and E. Pottier, "Multidimensional speckle noise model," *EURASIP Journal on Advances in Signal Processing*, vol. 2005, no. 20, p. 180956, Dec 2005. [Online]. Available: https://doi.org/10.1155/ASP.2005.3259

[24] S. N. Anfinsen, A. P. Doulgeris, and T. Eltoft, "Estimation of the equivalent number of looks in polarimetric synthetic aperture radar imagery," *IEEE Transactions on Geoscience and Remote Sensing*, vol. 47, no. 11, pp. 3795–3809, 2009.

[25] Yang Xiang, S. Gubian, B. Suomela, and J. Hoeng, "Generalized simulated annealing for efficient global optimization: the GenSA package for R." *The R Journal Volume 5/1, June 2013*, 2013. [Online]. Available: https://journal.r-project.org/archive/2013/RJ-2013-002/index.html

[26] V. Naidu and J. Raol, "Pixel-level image fusion using wavelets and principal component analysis," *Defence Science Journal*, vol. 58, no. 3, pp. 338–352, Mar. 2008. [Online]. Available: https://publications.drdo.gov.in/ojs/index.php/dsj/article/view/1653

[27] S. Giannarou and T. Stathaki, "Optimal edge detection using multiple operators for image understanding," *EURASIP Journal on Advances in Signal Processing*, vol. 2011, no. 1, p. 28, Jul 2011. [Online]. Available: https://doi.org/10.1186/1687-6180-2011-28

[28] T. Fawcett, "An introduction to roc analysis," *Pattern Recogn. Lett.*, vol. 27, no. 8, pp. 861–874, Jun. 2006. [Online]. Available: http://dx.doi.org/10.1016/j.patrec.2005.10.010